Journal of Molecular Structure 1234 (2021) 130169

Contents lists available at ScienceDirect

Journal of Molecular Structure

journal homepage: www.elsevier.com/locate/molstr

Inclusion of citral isomers in native and methylated cyclodextrins: Structural insights by X-ray crystallography and molecular dynamics simulation analysis

Katerina Fourtaka, Elias Christoforides, Pavlos Tzamalis, Kostas Bethanis*

Physics Laboratory, Department of Biotechnology, School of Applied Biology and Biotechnology, Agricultural University of Athens, 75 Iera Odos, Athens 11855, Greece

ARTICLE INFO

Article history:
Received 6 January 2021
Revised 8 February 2021
Accepted 13 February 2021
Available online 25 February 2021

Keywords:
Citral
α-Cyclodextrin
β-Cyclodextrin
Heptakis(2,6-di-*O*-methyl)-β-cyclodextrin
Heptakis(2,3,6-tri-*O*-methyl)-β-cyclodextrin
Inclusion complex
Crystal structure
Molecular dynamics

ABSTRACT

The crystal structure of the inclusion compounds of citral (*cr*) isomers in native α- and β-Cyclodextrin (α-CD and β-CD) as well as in heptakis(2,6-di-*O*-methyl)-β-cyclodextrin (DM-β-CD) and heptakis(2,3,6-tri-*O*-methyl)-β-cyclodextrin (TM-β-CD) have been explicitly investigated by X-ray crystallography and molecular dynamics (MD) simulations.

The *cr*/α-CD complex unit, with a 1:2 guest:host stoichiometry, consists of a head-to-head type α-CD dimer encapsulating either an *E*- or a *Z*-citral isomer with occupancy of 0.4 and 0.6 respectively. In the case of the *cr*/β-CD, head-to-head β-CD dimers are also formed, hosting two highly disordered guest molecules, both being *E*-citral isomers (2:2 guest:host stoichiometry). MD simulations based mainly on the determined crystal structures, show that the formed inclusion complexes are stable in a simulated aqueous environment and that *Z*-citral has the tendency to adopt a more 'bent' conformation than *E*-citral upon encapsulation in the hydrophobic CD cavity. MM/GBSA-calculations clearly indicate a higher binding affinity in the case of the *cr*/α-CD than the *cr*/β-CD inclusion complex.

The inclusion complexes of citral in DM-β-CD and TM-β-CD both crystallize with a 1:1 guest:host stoichiometry. Only the *E*-citral isomer is found inside the DM-β-CD with its aldehyde group protruding from the narrow rim of the host, whereas both *E*- and *Z*-citral isomers, with occupancy of 0,7 and 0,3 respectively, are present in the TM-β-CD accommodated with different modes inside the host's cavity. MD simulations in aqueous environment reveal a stable inclusion complex of citral in DM-β-CD and a rather unstable in TM-β-CD, the ascending order of the binding affinities of these inclusion complexes as estimated by MM/GBSA calculations being: *Z*/TMβCD < *E*/TMβCD < *E*/DMβCD.

It is noticed that in the crystalline state, the rigid cavity of β-CD and DM-β-CD favors the inclusion of the *E*-citral which adopts an extended conformation and is accommodated 'axially' in it, whereas the *Z*-citral isomer, that adopts a more bent conformation upon encapsulation in the hydrophobic CD cavity, is found only in the case of the *cr*/α-CD where the 1:2 guest:host stoichiometry provides the space to accommodate the bent *Z*-citral and in the case of the *cr*/TM-β-CD complex, where the bent *Z*-citral is found accommodated 'equatorially' near the wide secondary rim of the distorted host.

1. Introduction

Plant terpenoids, which are the main components of many natural herbal aromatic essential oils, comprise a class of isoprenoids that are well known for their pharmacological properties including antifungal, antibacterial, antioxidant and anticancer activities [1]. Citral (3,7-dimethyl-2,6-octadienal, *cr*) is a mixture of two geometric isomers (*E*-citral or geranial and *Z*-citral or neral, Fig. 1a), which provides an intense lemon odor during its application and is reported to have antimicrobial activity [2]. It is usually found in lemongrass oil, which has also been widely reported due to its microbicidal action that highlights it as a very useful "natural tool" with many applications in food and pharmaceutical industries [3–5]. Citral is a highly hydrophobic molecule and unstable

Abbreviations: citral (*cr*), alpha-cyclodextrin (*a*-CD); beta-cyclodextrin, (β-CD); heptakis(2,6-di-*O*-methyl)n, -β-cyclodextrin, (DM-β-CD); heptakis(2,3,6-tri-*O*-methyl)-β-cyclodextrinn, (TM-β-CD); Site occupancy factor, (sof); inclusion complex, (IC); molecular dynamics, (MD).

* Corresponding author.
E-mail address: kbeth@aua.gr (K. Bethanis).

https://doi.org/10.1016/j.molstruc.2021.130169
0022-2860/

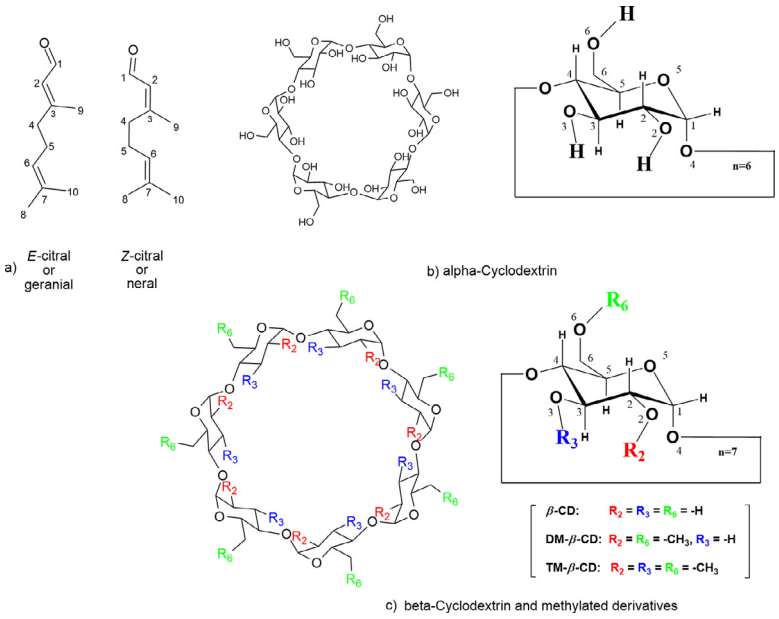

Fig. 1. Schematic representation of chemical structures of **(a)** *E*-citral and *Z*-citral isomers, **(b)** alpha-cyclodextrin (α-CD) and **(c)** beta-cyclodextrin (β-CD), heptakis(2,6-di-*O*-methyl)-β-cyclodextrin (DM-β-CD) and heptakis(2,3,6-tri-*O*-methyl)-β-cyclodextrin (TM-β-CD).

under normal storage conditions thus it can easily lose its activity [6]. Moreover, Adukwu *et al* have reported some concerns about the cytotoxicity of both pure citral and the lemongrass essential oil from *Cymbopogon flexuosus* [7]. An effective way to overcome these drawbacks is the formation of inclusion compounds of citral in Cyclodextrins (CDs), the well-known oligosaccharides composed of α-(1,4)-linked glucopyranose subunits (Fig. 1b and c), having the ability, due to their conical shape and amphiphilic nature (relatively hydrophilic external surface and hydrophobic interior cavity), to encapsulate a wide range of hydrophobic molecules (or molecules with hydrophobic parts) of appropriate size and scheme [8]. *a* -cyclodextrin (*a*-CD) and β-cyclodextrin (β-CD) are the well-known native CDs composed by 6 and 7 glucoses respectively (Fig. 1b and c), while the heptakis(2,6-di-*O*-methyl)-β-cyclodextrin (DM-β-CD) and heptakis(2,3,6-tri-*O*-methyl)-β-cyclodextrin methylated (TM-β-CD) are methylated derivatives of the parental β-CD (Fig. 1c).

The inclusion of citral isomers in native and modified CDs has been extensively characterized by various methods including ^{1}H-NMR, FT-IR, UV-Vis spectrophotometry, circular dichroism spectroscopy, XRD, DSC, TG/DTG, phase solubility (Higuchi-Connors), static headspace gas chromatography [9–17], and further studied by molecular modelling (Molecular Mechanics calculations and molecular dynamics simulations based on models constructed by docking with varying mole ratios) [16–18]. The morphology of the freeze dried solutions of the citral/CD inclusion complexes has been observed by TEM and SEM [12,14]. The general conclusion of all these studies is that the inclusion of citral in various CDs exerts beneficial effects on its physicochemical properties, namely: it prevents heat degradation of citral, improves its stability during long term storage and provides slow release that can be controlled by choosing appropriate native CDs or CDs derivatives. Moreover, recent studies have demonstrated important applications of citral/CD inclusion complexes: the anti-hyperalgesic, anti-inflammatory effects of citral/CD in mice [14] is of interest for the pharmaceutical industry; a new technique to produce aromatic cotton with control fragrance release by loading citral/CD in fibers [15] for the textile industry; the facile production of citral/CD nanofibers offering enhanced water solubility of citral along with high-temperature stability and longer shelf-life [19] which is of interest for the food (or related bio applications) industry. However, no crystal structure of any citral/CD inclusion complex has been reported so far. The crystal structure determination and analysis of these inclusion complexes offers unique information and resolves any ambiguity about the exact host:guest stoichiometry, the inclusion geometry, the intra- and inter-molecular interactions and the molecular arrangement of the complex units in the crystalline state.

In an ongoing investigation of cyclodextrin inclusion complexes with linear monoterpenoids [20,21], we present here the crystal structures of the inclusion complexes of citral in native α- and β-CD (*cr*/α-CD and *cr*/β-CD), and in methylated DM-β-CD and TM-β-CD (*cr*/DM-β-CD and *cr*/TM-β-CD) as determined by Single Crystal X-ray Diffraction (SCXRD). The four new structures are described in detail and they are compared with previously reported crystal structures of inclusion complexes of linear monoterpenoids like β-citronellol (*cl*), geraniol (*gr*) and linalool (*ln*) in similar CDs [20–22]. Moreover, based mainly on the crystallographically determined stoichiometry and atomic coordinates, we investigate, by molecular dynamics (MD) simulations of 12 ns, the dynamic behavior of these four inclusion complexes in an aqueous environment and in the absence of crystal contacts. With this *in silico* investigation we aim to inspect the role of the conformational flexibility of the guest and the type of the host (cavity size, rigidity of the macrocycle, substituent groups) in the stability of these inclusion complexes. The binding affinities are also estimated by MM/GBSA calculations. Our understanding of the structural details and dynamic behavior of the linear monoterpenoids upon complexation with CDs may be also useful in the engineering of modified guest-host systems with optimized properties and future practical applications.

2. Materials and methods

2.1. Materials

Citral as a clear yellow liquid mixture of geranial and neral (95% pure, d = 0.888 g/mL) was purchased from Sigma-Aldrich Co. LLC. α-CD and β-CD of pharmaceutical grade quality were obtained from Cyclolab (Budapest, Hungary), while DM-β-CD and TM-β-CD ($\geq$98% pure) as white powders from Sigma-Aldrich Co. LLC. Absolute ethanol (EtOH, > 99.8%) and distilled water were also obtained

from Sigma. All chemicals were used as received without further purification.

2.2. Preparation and crystallization of citral inclusion complexes in α-CD, β-CD, DM-β-CD and TM-β-CD

42μL of citral ethanolic solution (10% v/v) and 5mL of an equimolar aqueous solution of α-CD (0.25 mmol, 0.05M) were mixed and the mixture was stirred in a tightly sealed glass vial for 1 h at 70°C. Similarly, 13μL of citral and 5mL of an equimolar aqueous solution of β-CD (0.08 mmol, 0.016M) were mixed and the mixture was also stirred for 1 h at 70°C. The two mixtures allowed to cool gradually to room temperature over a period of one week, according to the slow cooling crystallization technique, until colorless transparent prismatic crystals in both cases were formed. Crystals of citral/DM-β-CD and citral/TM-β-CD inclusion complexes were prepared by adding isomolar amounts of host (44.00 mg or 0.033 mmol of DM-β-CD; 44.17 mg or 0.033 mmol of TM-β-CD) and guest (125 μL of citral) in 2 mL of distilled water. The two final mixtures were stirred vigorously at room temperature for 45 min and subsequently maintained at 321 K for a period of two weeks. Rod-shaped and prismatic crystals suitable for X-ray diffraction measurements were produced in the case of *cr*/DM-β-CD and *cr*/TM-β-CD, respectively.

2.3. X-ray data collection, structure solution and refinement

Intensity data for all complexes were collected on a Bruker D8-VENTURE diffractometer, using *Cu Ka* radiation (λ = 1.54178 Å) and deduced with the program *SAINT* [23]. Absorption correction was performed with *SADABS* [24]. The structures of the citral inclusion complexes in native CDs and in TM-β-CD were solved by Patterson-seeded dual-space recycling with the SHELXD program [25]. The structure of the citral/DM-β-CD inclusion complex was solved by molecular replacement, using the atomic coordinates of the DM-β-CD macrocycle of the 2,2′-bithiophene/DM-β-CD complex [26]. The molecular replacement solution was obtained by a Patterson vector search and Fourier recycling using the DIRDIF99 package [27]. The refinement of all crystal structures was performed by full-matrix least squares against F^2 using *SHELXL-2014/7* [28] through the *SHELXLE GUI* [29]. Soft restraints on bond lengths and angles, as provided by the PRODRG2 webserver [30], were applied only to model the disordered guest molecules. Anisotropic displacement parameters for citral atoms were refined with both soft (SIMU) and enhanced rigid bond (RIGU) restraints implemented in the *SHELXL* program [31]. All H-atoms of the host molecules were placed geometrically and allowed to ride on the parent atoms. *U*iso(H) values were assigned in the range 1.2–1.5 times *U*eq of the parent atom. In order to maintain a high (>7.0) data/parameters ratio, anisotropic thermal parameters were imposed to selected, non-H atoms of the host molecules. Mercury 4.1.3 [32] and Olex2 v1.2 [33] were used for geometrical analysis and to produce figures illustrating the crystal structures. Experimental details along with refinement statistics are quoted in Table 1. Crystallographic information files with embedded structure factors have been deposited into the Cambridge Structural Database (CSD).

2.4. Molecular dynamics

The MD simulations were based on the following initial models: For the citral/α-CD inclusion complex, the crystallographically determined atomic coordinates of the α-CD dimer and the sites occupied by the *E*- and *Z*-citral were used to comprise two distinct initial sets: *E*-citral/α-CD (*E*/αCD) and *Z*-citral/α-CD (*Z*/αCD), both of 1:2 guest:host stoichiometry. For the citral/β-CD inclusion complex, the crystallographically determined structure (2:2 guest:host stoichiometry), that consists of a β-CD dimer hosting two *E*-citral guests (*EE*/βCD) was used as an initial set of atomic coordinates. However, in order to examine the stability of possible dimeric β-CD inclusion complexes (of 2:2 guest:host stoichiometry), hosting a *Z*- and an *E*-citral (*EZ*/βCD) or two *Z*-citral guests (*ZZ*/βCD), two more initial sets, obtained by molecular modelling using Autodoc Vina [34], were used. For the inclusion complexes of citral in methylated CDs, based on the crystallographically determined atomic coordinates of the hosts and the found guests, the three initial models (all with an 1:1 guest:host stoichiometry) of *E*-citral/DM-β-CD (*E*/DMβCD), *E*-citral/TM-β-CD (*E*/TMβCD) and *Z*-citral/TM-β-CD (*Z*/TMβCD) were used.

All computations were performed using the Amber12 software package [35]. The Clycam06 [36] or the q4md-CD force field [37] were used to generate the correct native and modified CD topologies, respectively. The MD calculations were performed on a 24 core Intel Xeon 2.8GHz workstation with 32 GB internal memory.

Partial atomic charges and geometrical and topological parameters for citral were assigned by the ANTECHAMBER program [38] using the general AMBER force field (GAFF) parameters and the AM1-BCC methodology. Each complex was solvated in a periodic, 10-Å truncated octahedron simulation box consisted of TIP3P waters with the minimum distance of 10.0 Å from the system surface. All hydrogen atoms added by the xLEaP module were equilibrated by energy minimization of the system with 500 steps of the steepest descent method followed by 1000 steps of the conjugated gradient method to release the bad contact. Both minimization and MD calculations were performed with SANDER. The Particle Mesh Ewald method was employed to account for long range electrostatic interactions, while the nonbonded cutoff distance was set to 10 Å and all covalent bonds involving hydrogen atoms were treated by the constraint algorithm SHAKE [39]. Finally, a 12 ns MD production run with constant pressure of 1 atm and temperature of 300 K (NPT ensemble) was performed for all IC models using a time step of 1 fs. The detailed simulation protocol has been analytically described in a previous work [40]. The programs CPPTRAJ [41] and VMD [42] were used for data handling, processing, analyzing and visualizing.

The well-known MM/GBSA method [43] is a post-processing approach to estimate the binding free energy of molecules in solution, which combines the molecular mechanical (MM) energies (force fields) with continuum solvation models (Generalized-Born model and surface area continuum solvation method (GBSA)). Thus, this method was adopted here for calculating the binding free energy $\Delta G_{(GB)}$ of the inclusion complexes as the energy difference between the bound and unbound state of the solvated CD and citral molecules. The entropic penalty (ΔS) incurred upon guest binding is calculated by extracting snapshots from the MD trajectories every 100 frames using the NMODE module of AMBER and added to the enthalpic term according to (1):

$$\Delta G_{bind} = \Delta G_{(GB)} - T \cdot \Delta S \quad (1)$$

3. Results and discussion

3.1. Description of the crystal structures

3.1.1. The structure of citral/α-CD inclusion compound

The citral/α-CD inclusion complex crystallizes in *P*1 space group. Its asymmetric unit contains two α-CD host molecules (host A and host B), one citral guest molecule, nine waters and one ethanol molecule. The two host molecules are arranged co-axially forming a head-to-head dimer via a hydrogen bond net between

Table 1
Crystallographic data and structure refinement parameters for the citral/α-CD, citral/β-CD, citral/DM-β-CD and TM-β-CD inclusion complexes.

	citral/α-CD	citral/β-CD	citral/DM-β-CD	citral/TM-β-CD
Crystal data				
Chemical formula	$2(C_{36}H_{60}O_{30})\bullet C_{10}H_{16}O\bullet C_2H_6O\bullet 9(H_2O)$	$C_{42}H_{70}O_{35}\bullet C_{10}H_{16}\bullet$ 6.65(H_2O)	$C_{56}H_{98}O_{35}\bullet C_{10}H_{20}O\bullet$ 0.6(H_2O)	$C_{63}H_{112}O_{35}\bullet C_{10}H_{20}O\bullet$ 1.2(H_2O)
M_r	2287.97	2787.21	1491.57	1599.94
Crystal system, space group	Triclinic, *P*1	Monoclinic, *C*2	Orthorhombic, $P2_12_12_1$	Orthorhombic, $P2_12_12_1$
Temperature (K)	100	293	100	100
a, *b*, *c* (Å)	13.8115 (19), 13.8652 (16), 15.648 (2)	18.892 (4), 24.452 (4), 15.662 (5)	11.2400 (6), 14.9344 (8), 45.211 (2)	14.659 (2), 21.404 (3), 27.887 (4)
α, β, γ (°)	85.177 (12), 88.117 (10), 60.169 (10)	110.748 (15)		
V (Å^3)	2590.2 (6)	6766 (3)	7589.2 (7)	8750 (2)
Z	1	2	4	4
Radiation type	Cu *Kα*	Cu *Kα*	Cu *Kα*	Cu *Kα*
μ (mm^{-1})	1.13	1.05	0.90	0.82
Crystal size (mm^3)	0.35 × 0.2 × 0.1	0.3 × 0.22 × 0.15	0.8 × 0.4 × 0.2	0.8 × 0.4 × 0.2
Data collection				
Diffractometer	Bruker *APEX*-II	Bruker *APEX*-II	Bruker *APEX*-II	Bruker *APEX*-II
T_{min}, T_{max}	0.444, 0.754	0.621, 0.752	0.582, 0.753	0.243, 0.753
No. of measured, independent and observed [$I > 2\sigma(I)$] reflections	96926, 19920, 19719	38253, 11318, 9902	67543,10479, 10055	68931, 15345, 13185
R_{int}	0.040	0.035	0.042	0.070
$(\sin\theta/\lambda)_{max}$ (Å^{-1})	0.626	0.588	0.562	0.596
Refinement				
$R[F^2 > 2\sigma(F^2)]$, $wR(F^2)$, *S*	0.042, 0.115, 1.05	0.053, 0.148, 1.02	0.085, 0.235, 1.24	0.109, 0.267, 1.09
No. of reflections	19920	11318	10479	15345
No. of parameters	1452	928	912	1214
No. of restraints	44	108	42	175
$\Delta\rho_{max}$, $\Delta\rho_{min}$ (e Å^{-3})	0.51, -0.44	0.42, -0.29	0.51, -0.60	0.57, -0.65
CCDC deposition number	1854912	1831155	2019612	2022366

their secondary hydroxyl groups as the wide rim of the one faces the wide rim of the other. Inside the formed dimeric cavity, a citral molecule is encapsulated, therefore the guest:host stoichiometry of the inclusion complex in the crystalline state is 1:2. In about 60% of the inclusion complex units, the *Z*-isomer of citral (*Z*-citral or neral) is found encapsulated, whereas in the rest 40% of the inclusion complex units, the *E*-isomer of citral (*E*-citral or geranial) is hosted in the α-CD dimer. The inclusion mode is the same for both *E*- and *Z*-citral guests: The alkenyl group (atoms C6, C7, C8, C10; see Fig. 1a) of both isomers occupies the same atomic positions, located inside the hostA cavity. Two hydrogens of the C10 methyl group and the hydrogen of the C6 atom form closed shell interactions with the inner H3 atoms of the hostA hydrophobic cavity (**Supplementary Table S1-I**). The rest of the aliphatic tail of the guest is extended axially towards the interface of the α-CD dimer and the encapsulated citral isomers are further stabilized by CH … O bonds formed with the secondary hydroxyls of the hostA and closed shell interactions with the inner H3 and H5 atoms of both hosts (A and B) which form the dimer (**Supplementary Table S1-I**). The aldehyde group of both encapsulated *E*- and *Z*-isomer is hydrogen bonded with an ethanol molecule that is found disordered over 3 sites and it is accommodated in the interspace of the adjacent α-CD dimers that form channels along the crystallographic *c*-axis as described below (Fig. 2a and b; **Supplementary Table S1-I**). The nine water molecules of the asymmetric unit (one of them is found disordered over two sites) are located around the α-CD dimer, close to the primary and secondary rims of the cyclodextrins, bridging via hydrogen bonds the adjacent complex units along the *a*- and *b*- crystallographic axes (Fig. 2b).

Geometrical features defining the conformation of the *a*-CD molecules are listed in the **Supplementary Table S2-I**. The glucosidic O4*n* atoms in both host molecules form nearly regular hexagons which are essentially planar as indicated by the distances of the O4*n* atoms from their approximate centroids and their deviations from the O4*n* mean plane. The glycosidic residues have positive tilt angles indicating that their primary sides incline towards the approximate sevenfold axis of the cavity. All the primary hydroxyl groups of the host have the *gauche-gauche (gg)* conformation pointing outwards the cavity and being hydrogen bonded with the surrounding water molecules. These water molecules are also hydrogen bonded with the primary rim of the consecutive dimer along the *c*-axis, bridging the complex units that stack in a chan-

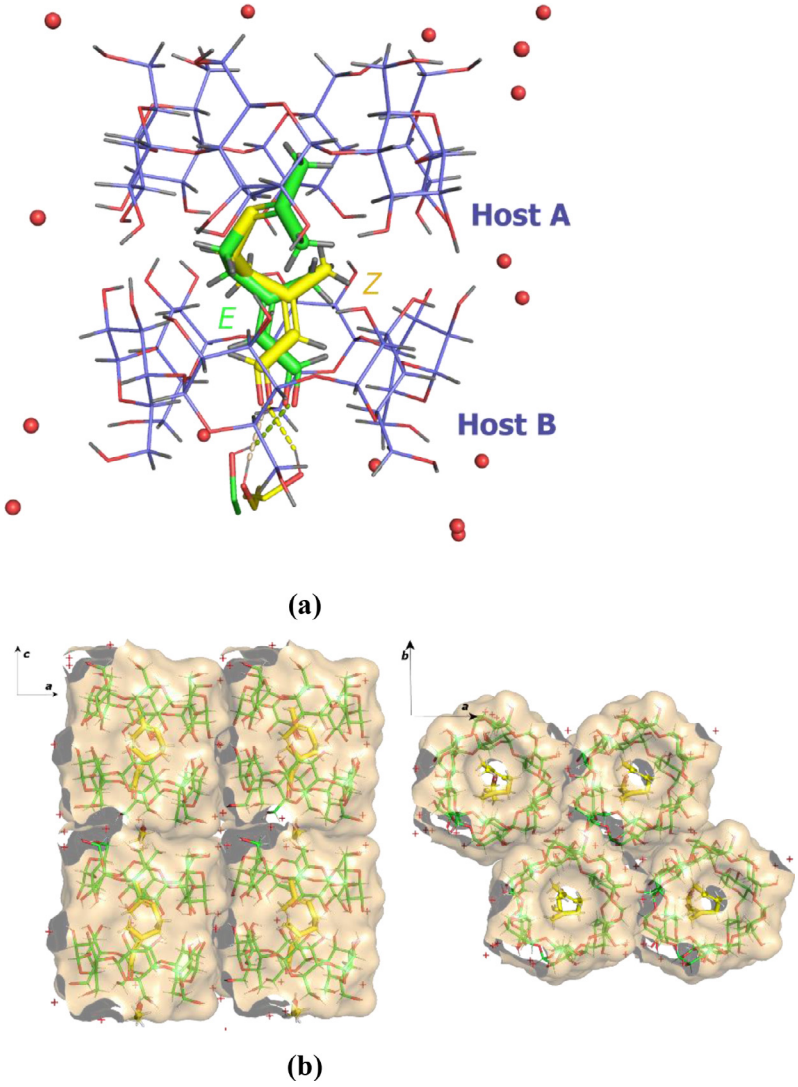

Fig. 2. **(a)** The asymmetric unit of the citral/α-CD crystal structure comprises of a head-to-head α-CD dimer encapsulating a citral molecule (1:2 guest:host stoichiometry). Both *E*- and *Z*-citral isomers (depicted as green and yellow, respectively) are present as distinct sites of one disordered citral guest molecule with occupancy factors of 0.4 and 0.6 respectively. An ethanol molecule disordered over 3 sites is also located near the primary rim of host B, hydrogen bonded with the aldehyde group of the citral and **(b)** citral/α-CD complex units form channels along the *c*-axis (left) and layers on the *ab* plane (right). Only one citral isomer guest is depicted for clarity.

nel mode. The shift between successive dimers along the *c*-axis is 2.05 Å while their approximate six-fold axis form an angle of 8.5° with the *c*-axis. The adjacent α-CD dimers on the *ab* plane form layers, as they are also interconnected either directly via hydrogen bonds between their secondary hydroxyls or indirectly via hydrogen bonds with bridge water molecules close to their primary and secondary rim (**Supplementary Table S1-I,** Fig. 2b).

A Cambridge Structural Database (CSD) [44] search based on similar cell dimensions resulted in 9 isostructural inclusion compounds and 2 clathrates of α-CD that crystallize in the triclinic space group and in the same molecular packing. Specifically, the inclusion complex of diethyl fumarate/α-CD (CIGLAG) [45] and butyl-isothiocyanate/α-CD (XIGBOE) [46] form alternatively head-to-head and tail-to-tail dimers (clathrates) as the guest molecule is located in the interspace between two adjacent tail-to-tail α-CDs. All the other structures form head to head dimers (inclusion complexes), the guest molecules of the inclusion complexes being fully encapsulated inside the dimeric cavities as in the present case of the citral/α-CD inclusion complex.

3.1.2. The structure of citral/β-CD inclusion compound

The citral/β-CD inclusion complex crystallizes in *C2* space group and its asymmetric unit contains one β-CD host molecule, one citral guest molecule and 7 water molecules distributed over 19 sites.

The guest citral molecule is encapsulated axially in the host's cavity with its aldehyde group protruding from the primary rim of the β-CD. The guest is found highly disordered in the β-CD cavity, occupying three sites, noted as *cr*1, *cr*2 and *cr*3 with occupancy factors of 0.3, 0.3 and 0.4 respectively. All three occupied sites correspond to the *E*-citral configuration and they form closed-shell interactions with the inner H3 and H5 atoms of the host's cavity. Moreover, in the case of *cr*1, CH…O bonds between the hydrogens of C4 of the guest and the glycosidic oxygen O4 of the 7th glucopyranose unit (G7) of the β-CD is observed, whereas in the case of *cr*3, the aldehyde oxygen of the guest forms a hydrogen bond with a primary hydroxyl of the β-CD (**Supplementary Table S1-II**). The twofold symmetry-related molecular complexes form head-to-head dimers via the usual intermolecular hydrogen bonds between the

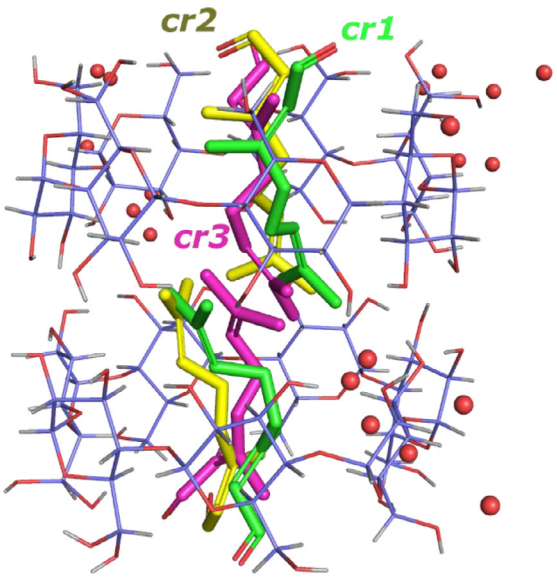

(a)

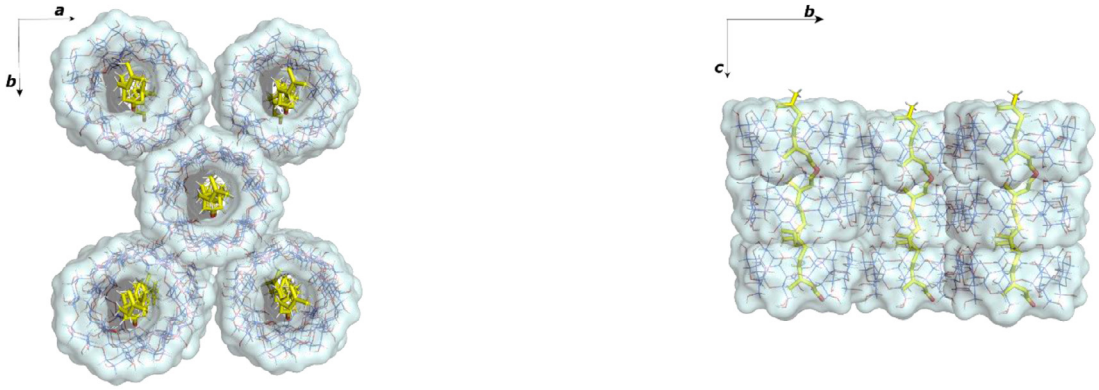

(b)

Fig. 3. **(a)** The citral/β-CD inclusion complex forms head-to-head dimers with a guest:host stoichiometry of 2:2 surrounded by a disordered water network. Only the *E*-configuration of citral is found inside the β-CD cavity. The guest is disordered over three sites (*cr*1, *cr*2 and *cr*3). Hydrogen atoms of the guest molecule are omitted for clarity. **(b)** (left) projection of the crystal packing along *c*-axis and **(**right**)** projection of the crystal packing along *a*-axis. β-CD dimers form channels along the *c*-axis and layers along the *ab* plane.

O3*n*H secondary hydroxyl groups of the twofold symmetry-related β-CDs. The two *E*-citral molecules hosted inside the dimeric cavity, are accommodated with the alkenyl group of their aliphatic tale located in the interface of the dimer, facing each other and forming closed shell interactions between each other. Due to steric reasons, the guest-duets existed in the dimeric cavity are: *cr*1-*cr*1, *cr*1-*cr*2, *cr*1-*cr*3 and *cr*2-*cr*3. In any case, the actual guest:host stoichiometric ratio of the inclusion complex in the crystalline state is 2:2 (1:1) (Fig. 3a).

The conformation of the host β-CD molecules is described by the geometrical features listed in the **Supplementary Table S2-II**. The reference glycosidic O4*n* atoms of the host form nearly planar and regular heptagons whereas all the glycosidic residues incline towards the primary rim. The primary hydroxyl groups of the host have the *gauche-gauche (gg)* conformation pointing outwards the cavity and being hydrogen bonded with bridge water molecules. However, three of them, which are disordered over two sites each, also adopt the *gauche-trans (gt)* conformation as they are hydrogen bonded with the guest or a primary hydroxyl of the adjacent dimer. Specifically, *gt* conformation is observed for the partially occupied site2 of the primary hydroxyl of the G5 glucopyranose unit which is hydrogen bonded with the O1 atom of the guest occupying the *cr*3 site, and for the partially occupied sites of the primary hydroxyls of the G2 and G6 glucopyranose units that form hydrogen bonds between each other in the shifted adjacent dimers that are piled up to columns along the *c*-axis (**Supplementary Table S1-II**).

Each dimeric unit is replicated by twofold rotation symmetry along the *b*-axis and thus the dimers are arranged according to the Channel (*CH*) packing mode [47] as their approximate seven-fold axis forms an angle of 89.95(15)° with the *c*-axis and the shift between successive dimers along the *c*-axis is 2.82(9) Å (Fig. 3b). The host β-CD molecules of consecutive dimers in the channel are interoconnected directly via hydrogen bonds formed

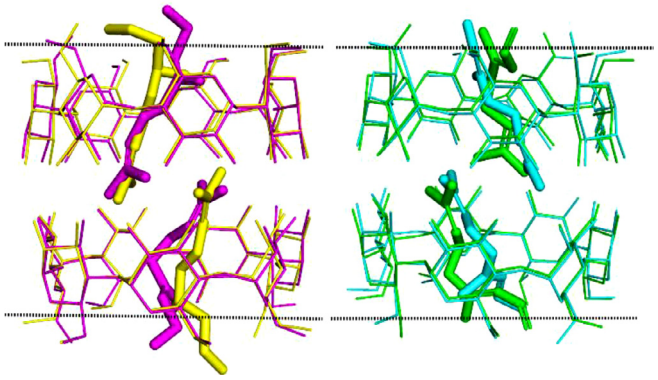

Fig. 4. (Left) Superpose of *β-citronellol*/*β*-CD (yellow) and *geraniol*/*β*-CD form I (magenta) inclusion complexes, reveals a relatively high protrusion of the guests from the narrow CD rims that inhibits the formation of channels in the crystalline state. (Right) Guests in *geraniol*/*β*-CD form II (cyan) and citral/*β*-CD (green) are encapsulated deeper in the CD dimers aiding the formation of channels.

between their primary hydroxyls or indirectly via hydrogen bonds with bridge water molecules. The guest *E*-citral molecules of consecutive dimers in the channel, accommodated with their aldehyde group protruding from the primary rim of the hosts as mentioned above, form CH …O bonds between each other, namely: the O1 of the site *cr*1 (x, y, z) with the H-C2 of the site *cr*2 or H-C10 of the site *cr*3 occupied by the guest of the consecutive dimer (1-x, y, 1-z). Any other combination of occupied sites of guests in consecutive dimers is sterically forbidden. The neighboring channels are bridged directly or indirectly (via bridge water molecules) via hydrogen bonds forming layers of dimeric inclusion complexes along the *ab* crystal plane (Fig. 3b).

A CSD [44] search for crystal structures of similar cell dimensions, revealed 37 isostructural inclusion complexes and clathrates of *β*-CD. By limiting the survey to inclusion complexes of linear terpenoids in *β*-CD, we found that the crystal structures of linalool/*β*-CD [48], *β*-citronellol/*β*-CD [20] and geraniol/*β*-CD form I [49] and form II [21] have been previously reported. The guests in all these inclusion complexes are encapsulated in *β*-CD dimers with the same stoichiometry and inclusion mode as the one observed in the citral/*β*-CD structure presented here, highlighting the tendency for the formation of linear monoterpenoids inclusion complexes in *β*-CDs with an 2:2 guest:host.soichiometry and in a specific inclusion mode.

However, an intermediate (*IM*) mode of crystal packing is observed in the cases of *β*-citronellol/*β*-CD and geraniol/*β*-CD (form I) inclusion complexes, whereas citral/*β*-CD, geraniol/*β*-CD (form II) and linalool/*β*-CD form channels (*CH* packing mode) in the crystalline state. This is due to the different degree of protrusion of the guests from the narrow *β*-CD rims that inhibits or allows the formation of channels by the dimeric complex units in the crystalline state [21] (Fig. 4).

3.1.3. The structure of citral/DM-β-CD inclusion complex

The inclusion complex crystallizes in the orthorhombic space group $P2_12_12_1$ and its asymmetric unit contains one host molecule, one *E*-citral guest molecule and a half-occupied water molecule disordered over two sites. The water occupied sites are located at H-bond distances from the hosts of adjacent complex units (**Supplementary Table S1-III**). The encapsulated *E*-citral is found inside the DM-*β*-CD cavity with its aldehyde group protruding from the narrow rim of the host and its lipophilic chain extending throughout the cavity towards the wide rim of the host (Fig. 5a). The oxygen atom of the *E*-citral forms a CH … O bond with a disordered methoxy group of the host of the adjacent complex unit whereas the aliphatic part of the guest is stabilized by closed shell interactions with the inner hydrogen atoms of the host's hydrophobic cavity (**Supplementary Table S1-III**).

The summarized in **Supplementary Table S2-III** geometric features of the host, indicate a torus-like shape and a round conformation of the CD macrocycle that resembles a canonical heptagon, similar to that of *β*-CD in its complex with citral. Among the 4 fully occupied primary methoxy sites, 2 of them are found to have the *gt* and 2 the *gg* conformation, while the 3 disordered methoxy groups adopt both conformations (**Supplementary Table S2-III**). Thus, the host adopts an open cone conformation, which allows the entrance and exit of the guest molecules from both its wide and narrow rim.

The inclusion complex units are arranged according to a cage-type mode in the crystal, satisfying the self-inclusion tendency of the host DM-*β*-CD (Fig. 5a). The mean plane of the O4*n* atoms of the host forms an angle of 36.18(9)° with the crystallographic *bc* plane and an angle of 72.36(16)° with the O4*n* atoms mean plane of the host of an adjacent (-0.5+x, 0.5-y, -z) complex unit. The wide rim of the host is intruded by two secondary methoxy groups (those of the 1st and 7th glucopyranose units) of this adjacent complex unit and by two primary methoxy groups (of the 6th and 7th glucopyranose units) of the host of the neighboring complex unit along the *a*-axis (-1+x, y, z).

A CSD search for crystal structures of similar unit cell, resulted in two DM-*β*-CD inclusion complexes (refcodes: XIXKUL and COFLOY) that crystallize in the same space group ($P2_12_12_1$). The XIXKU structure is a clathrate of 2,2′-bithiophene with DM-*β*-CD [26] crystallizing with the similar cage-type crystal packing, whereas no crystal packing information could be found for the COFLOY structure which is the acetate-meta-toluene inclusion complex in DM-*β*-CD [50].

3.1.4. The structure of citral/ TM-β-CD inclusion complex

The citral/TM-*β*-CD inclusion complex crystallizes in the orthorhombic space group $P2_12_12_1$. The asymmetric unit consists of one TM-*β*-CD encapsulating one citral molecule. *E*-cital is found with an occupancy factor of 0.7 whereas *Z*-citral with 0.3. *E*-cital is accommodated almost axially inside the hydrophobic cavity of the host with its aldehyde group towards the rim of the primary methoxy groups of TM-*β*-CD and its aliphatic tail protruding from the secondary methoxy rim of TM-*β*-CD. On the other hand, *Z*-citral is found in a rather bent conformation, equatorially oriented along the wide rim of the host. The aliphatic tail and the aldehyde group of the *Z*-citral both protrude from the secondary methoxy rim of the host, the latter being hydrogen bonded with a water molecule located in the interspace of the complex units. This water molecule, having the same occupancy with *Z*-citral (0.3), participates in a network of 4 partially occupied water molecule sites (s.o.f = 0.3 for each one) that bridges the adjacent complex units (Fig. 5b). In any case, the guest occupying either the *E*- or the *Z*-citral site, it is stabilized by closed shell interactions and CH … O bonds with the encapsulant TM-*β*-CD, and by closed shell interactions with the host of the consecutive complex unit (1-x, -0.5+y, 0.5-z) in the formed column (described below) along the crystallographic *b*-axis (**Supplementary Table S1-IV).**

As it has been observed in almost all the structures of inclusion complexes in TM-*β*-CD reported so far, the macrocycle of the host molecule in *cr*/TM-*β*-CD is severely distorted due to the absence of intramolecular hydrogen bonds between the secondary methoxy groups of the host and the induced-fit mechanism for the inclusion complex formation. According to the geometrical features given in the **Supplementary Table S2-IV** (see also **Supplementary Figure S1**), the etheric O4*n* atoms that link the cyclodextrin residues with each other form an elliptical heptagon with its long axis in the di-

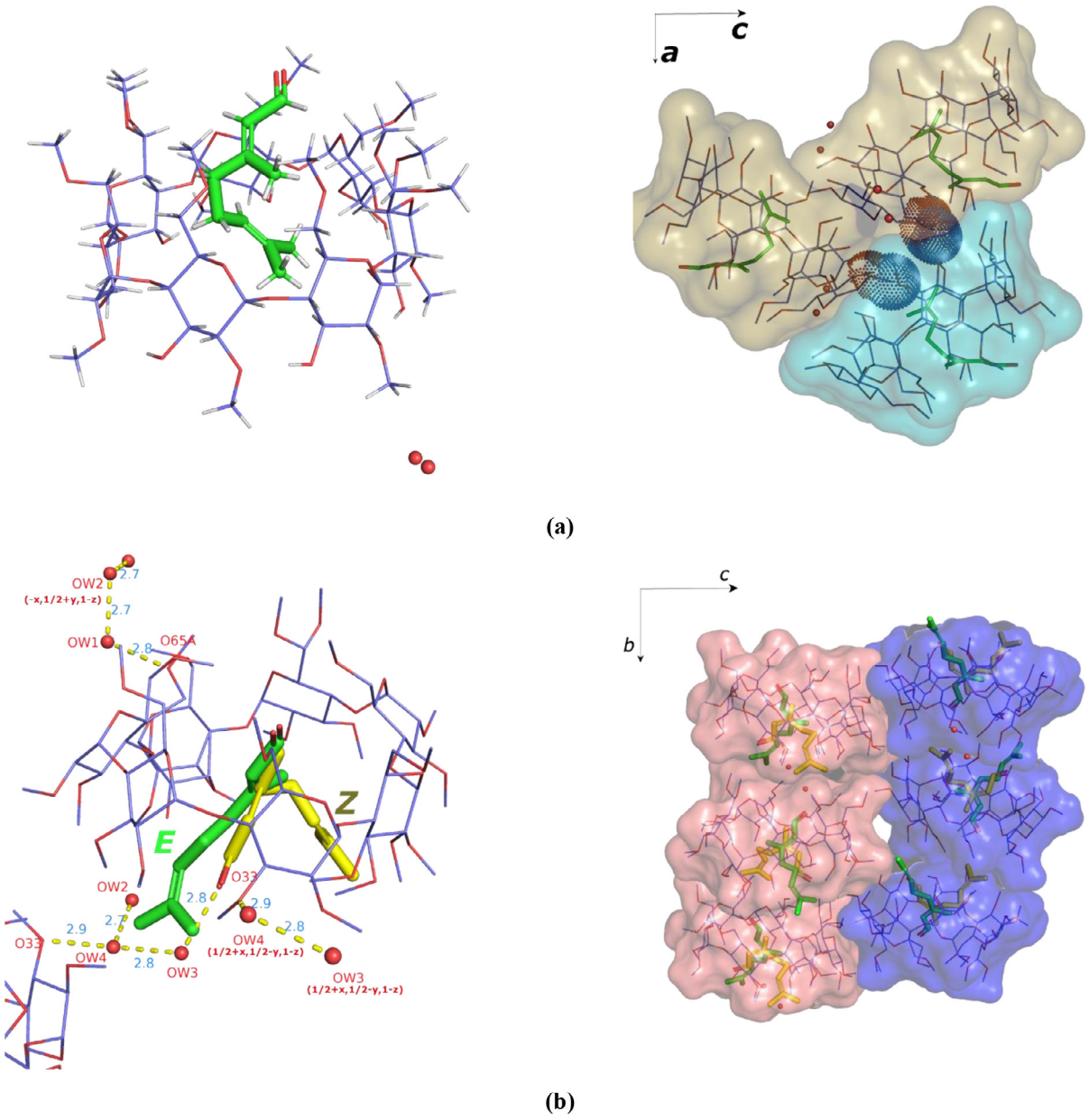

Fig. 5. **(a)** (Left) The inclusion complex of *cr*/DM-β-CD forms monomers with guest:host stoichiometry of 1:1. Only the *E*-citral isomer (green, sof 1.0) is present inside the CD cavity. (Right) Crystal packing projection along the *a*-axis. Inclusion complex units are arranged according to a cage-type mode satisfying the self-inclusion tendency of DM-β-CD and **(b)** (left) the inclusion complex of *cr*/TM-β-CD forms monomers in a guest:host stoichiometry of 1:1. The *E*-citral isomer (green, sof 0.7) has an 'axial' orientation, whereas the *Z*-citral isomer (yellow, sof 0.3) is accommodated 'equatorially' inside the cavity hydrogen bonded with bridging water molecules. (Right) The crystal packing of the *cr*/TM-β-CD complex: inclusion complex units form columns along the *b*-axis and antiparallel columns are packed along the *c*-axis.

rection of the equatorially accommodated *Z*-citral. Five out of the seven glucose units of the host illustrate positive tilt angles (dihedral angle between the O4*n* mean plane and the mean plane of the O4(*n*-1), C1*n*, C4*n* and O4*n* atoms) pointing towards the interior of the cyclodextrin macrocycle, while the other two point towards its exterior. The conformation of the primary methoxy groups of the host, as it is indicated by the O5*n*-C5*n*-C6*n*-O6*n* torsion angles, is gauche-gauche (*gg*) for all residues, except for those of G1 and the partially occupied sites of G5 (sof = 0.5) and G7 (sof = 0.5) which adopt the gauche-trance (*gt*) conformation. The primary methoxy groups of G1, G5 and G7 form the characteristic "lid" at the primary rim of TM-β-CD that has been observed in the vast majority of TM-β-CD inclusion complex structures, forbidding the guest penetration through the primary rim and constraining its accommodation towards the secondary rim of the host [51].

The complex units of citral/TM-β-CD related by the crystallographic symmetry of the twofold screw axis parallel to the crystallographic *b*-axis are arranged in a head-to-tail mode forming columns (Fig. 5b). Parallel columns are packed along the direction of the *a*-axis whereas antiparallel columns are packed along the direction of the *c*-axis. This crystal packing is not rare for TM-β-CD inclusion complexes. A search in the CSD [44], based on unit cell similarities, resulted the following four entries of permethylated β-CD inlusion compounds that crystallize in the orthorhombic $P2_12_12_1$ space group forming columns along the *b*-axis: (i) 2-Chloro-N-(ethoxymethyl)-N-(2-ethyl-6-methylphenyl)acetamide/TM-β-CD (CIJVIC) [52], (ii) p-iodophenol/TM-β-CD (CAMPIP) [53], (iii) (S)-p-methoxyphenyl/TM-β-CD (SIBSIG) [54] and (iv) 3-cyclooctyl-1,1-dimethylurea/TM-β-CD (OYAPIO) [55]. The cases of CAMPIP and OYAPIO resemble that of

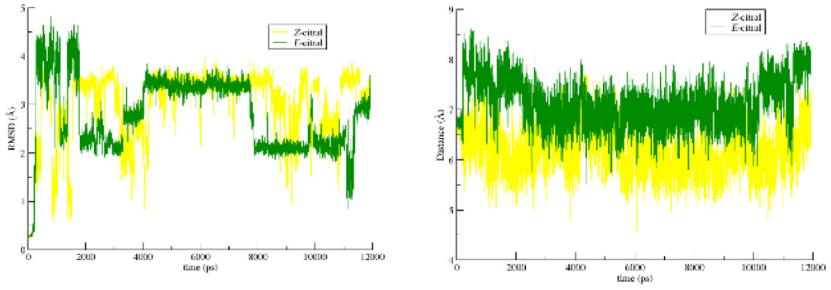

(a) **(b)**

Fig. 6. **(a)** RMSD over time for the two citral isomers in two distinct simulations (*E*/α-CD and *Z*/α-CD) and **(b)** the distance plot between the O and C7 atoms of the guest molecule in both *E*/α-CD and *Z*/α-CD inclusion complexes.

cr/TM-β-CD as the asymmetric unit of both crystal structures consists of one host, one guest and four water molecules bridging the adjacent complex units.

3.2. Molecular dynamics

3.2.1. Trajectory analysis for the citral/native-CD inclusion complexes

Based mainly on the crystallographically determined atomic coordinates, five independent simulations with different initial structures of citral/native-CD inclusion compounds were carried out at 300 K and in explicit water solvent for almost 12 ns as described in paragraph 2.4. More specifically, the cases of the inclusion complexes of *E*/α-CD and *Z*/α-CD with guest:host stoichiometry 1:2 and *EE*/β-CD, *EZ*/β-CD and *ZZ*/β-CD with guest:host stoichiometry 2:2, were studied.

In the cases of the *E*/α-CD and *Z*/α-CD inclusion complexes, the starting models correspond to head-to-head α-CD dimers encapsulating *E*- or *Z*-citral guest molecules respectively. MD simulations showed that, in both cases, the guest remains encapsulated inside the dimeric cavity without changing its orientation. By tracking the position and orientation fluctuations of the two isomers, *E*-citral seems slightly more stable inside the cavity. The root mean square deviations (RMSDs) over time from the crystallographically determined initial pose, are presented for the two guests in Fig. 6a. Moreover, the plot of the distance between the aldehyde group (O1 atom) and the isobutylenic group (C7 atom) of the guest in both *E*/α-CD and *Z*/α-CD complexes (Fig. 6b), indicates that, over the time frame of the MD simulations, *Z*-citral adopts a more bent conformation than *E*-citral inside the apolar environment of the dimeric α-CD cavity.

In order to estimate the binding affinity of the inclusion complexes, we assigned the two α-CD hosts as the receptor of the system and the citral isomer as the ligand. The results given in Table 2 indicate the formation, mainly via van der Waals interactions, of equally stable inclusion complexes in both cases.

For the inclusion complex of citral in native β-CD, although the crystallographic studies revealed the encapsulation of solely *E*-citral isomers inside the formed β-CD dimeric cavity with a 2:2 guest:host stoichiometry (*EE*/β-CD), we also investigated by MD simulations dimeric β-CD complexes hosting two *Z*-citral (*ZZ*/β-CD) as well as one *E*-citral and one *Z*-citral guest (*EZ*/β-CD).

In the *EE*/β-CD case, the examination of the dynamic behavior of the guests revealed their tendency to rotate about the sevenfold molecular axis of the hosts retaining their initial 'axial' orientation in a stable β-CD dimer during the 12 ns simulation (Fig. 7a). This dynamic behavior does not differ from that observed for citronellol/β-CD [20] and geraniol/β-CD [21] dimeric inclusion complexes. However, a totally different situation has been recorded in the other two cases: The *Z*-citral in the *EZ*/β-CD inclusion complex, flips over and it is found with its aldehyde group near the secondary rim of the respective host, adopting an 'equatorial' orientation. Similar behavior is observed for the one of the two guests in the ZZ/β-CD inclusion complex (Fig. 7a). This dynamic behavior is a result of the ability of *Z*-citral to adopt, unlike *E*-citral, bent conformations inside the hydrophobic environment of the β-CD cavity as in the case of the α-CD dimer (**Supplementary Figure S2**). The RMSDs from the first frame over time for the two guests in the three simulations were plotted and given in Fig. 7b. The observed variety of inclusion modes of *Z*-citral in the β-CD dimeric cavity probably explains why neither *EZ*/β-CD nor *ZZ*/β-CD inclusion complexes were found in the crystalline state: the presence of different building blocks may hinder the formation and growth of such crystals.

Table 2
Binding free energies and their standard deviations (kcal/mole) resulting from MM/GBSA analysis of the inclusion compounds of *E*-citral and *Z*-citral isomers in native α-CD (guest:host stoichiometry 1:2).

	E/α-CD	*Z*/α-CD
ΔE_{vdW}	-34.5 ± 1.7	-34.2 ± 1.7
ΔE_{ele}	-2.8 ± 2.6	-3.6 ± 2.2
ΔE_{GB}	16.5 ± 2.3	16.9 ± 1.8
ΔE_{surf}	-3.8 ± 0.1	-3.8 ± 0.1
ΔG_{gas}	-37.2 ± 2.9	-37.7 ± 2.5
ΔG_{solv}	12.7 ± 2.3	13.1 ± 1.8
$\Delta G_{(GB)}$[a]	-24.6 ± 2.0	-24.6 ± 2.0
$T\cdot\Delta S$	-17.0 ± 3.8	-17.1 ± 2.1
ΔG_{bind}[b]	**-7.6 ±4.3**	**-7.5 ± 2.8**

ΔE_{vdW} = van der Waals contribution from molecular mechanics
ΔE_{ele} = electrostatic energy as calculated by the molecular mechanics force field
ΔE_{GB} = the electrostatic contribution to the solvation free energy, calculated by G_B model
ΔE_{surf} = nonpolar contribution to the solvation free energy, calculated by an empirical model
[a] $\Delta G_{(GB)} = \Delta G_{solv} + \Delta G_{gas}$
[b] $\Delta G_{bind} = \Delta G_{(GB)} + T\cdot\Delta S$

MM/GBSA analysis of the citral/β-CD inclusion complexes was performed as follows: the system consisting of the two β-CDs of the dimeric host and one of the two guests was used as a receptor, whereas the other encapsulated guest was used as a ligand, in each one of the *EE*/β-CD, *EZ*/β-CD and *ZZ*/β-CD cases. The results indicate the formation of stable inclusion complexes mainly via van der Waals interactions in all cases as the ΔG values are similar within the error margin of the method (Table 3). By comparing these values with those reported for the cases of β-citronellol/β-CD and geraniol/β-CD (form II) 2:2 inclusion complexes [20–21], we end up with the following ascending order for the stability of these inclusion complexes: *citral*/β-CD < *geraniol*/β-CD < *β-citronellol*/β-

CD. Moreover, we notice that the absolute values of ΔG estimated for the inclusion complexes of citral in β-CD (Table 3) are significantly lower than those estimated for the inclusion complexes of citral in α-CD (Table 2) clearly indicating a more stable *cr*/αCD inclusion complex under the guets:host stoichiometries revealed by the determined crystal structures.

3.2.2. Trajectory analysis for the citral/methylated-CD inclusion complexes

The crystallographically observed *E*/DMβCD, *E*/TMβCD and *Z*/TMβCD inclusion complexes were subjected to minimization and subsequent MD runs in order to examine the dynamic behavior of the *E*-citral in two different hosts (DM-β-CD and TM-β-CD) and the dynamic behavior of the *E*- and *Z*-citral isomers in the same host (TM-β-CD). The RMSD plot for the guest obtained by these simulations (Fig. 8a, left) indicates a higher mobility of the *E*-citral in the TM-β-CD than in the DM-β-CD cavity. Visual inspection of the trajectories shows that the guest *E*-citral remains encapsulated 'axially' inside the hydrophobic cavity of both hosts. However, DM-β-CD host retains always its open cone conformation, due to the intramolecular hydrogen bonds formed between its secondary hydroxyls and methoxy groups of the adjacent glucose units. The lack

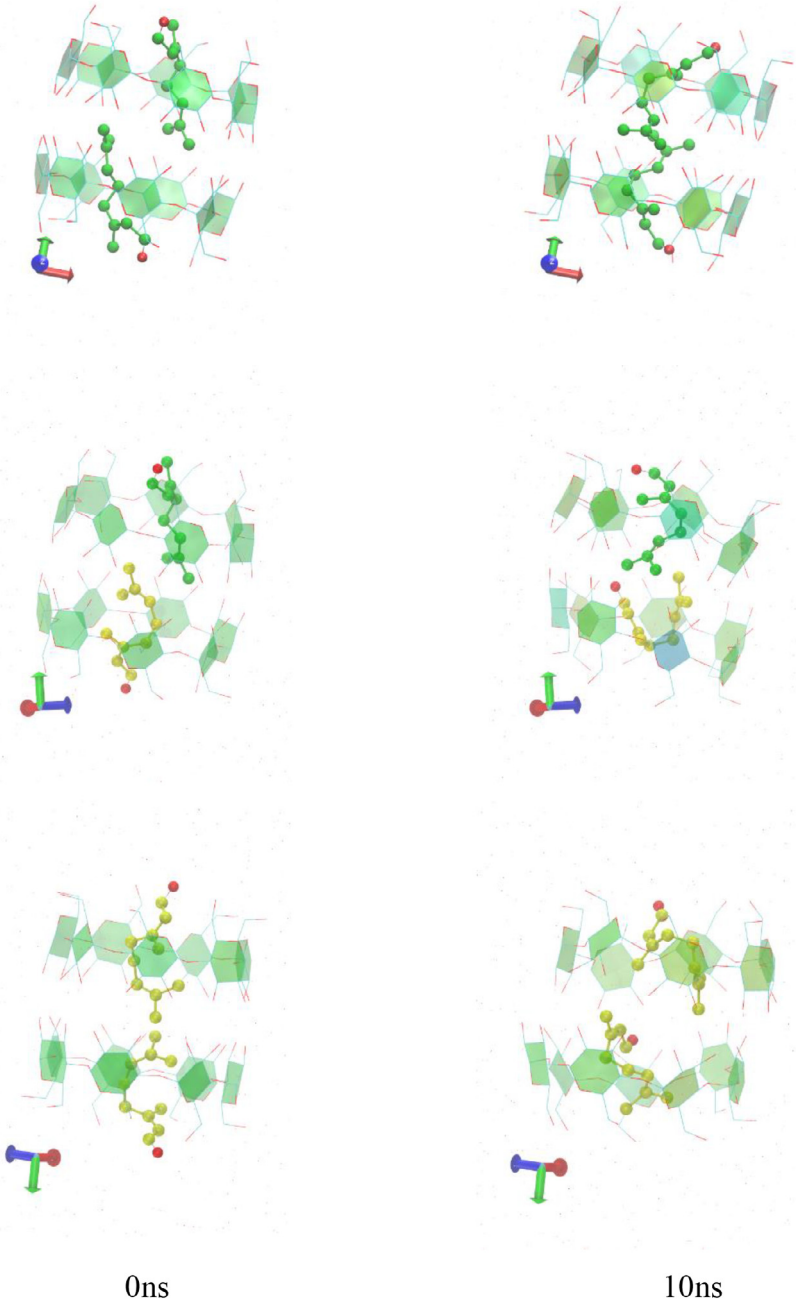

Fig. 7. **(a)** Representative snapshots at 0 and 10ns for *EE*/βCD, *EZ*/βCD and *ZZ*/βCD inclusion complexes (*E*-citral green; *Z*-citral yellow) shown as CPKs (guests) and paper chain (hosts), and **(b)** time evolution of RMSD for all non-H atoms of the two encapsulated citral isomers in each one of the three inclusion complex cases.

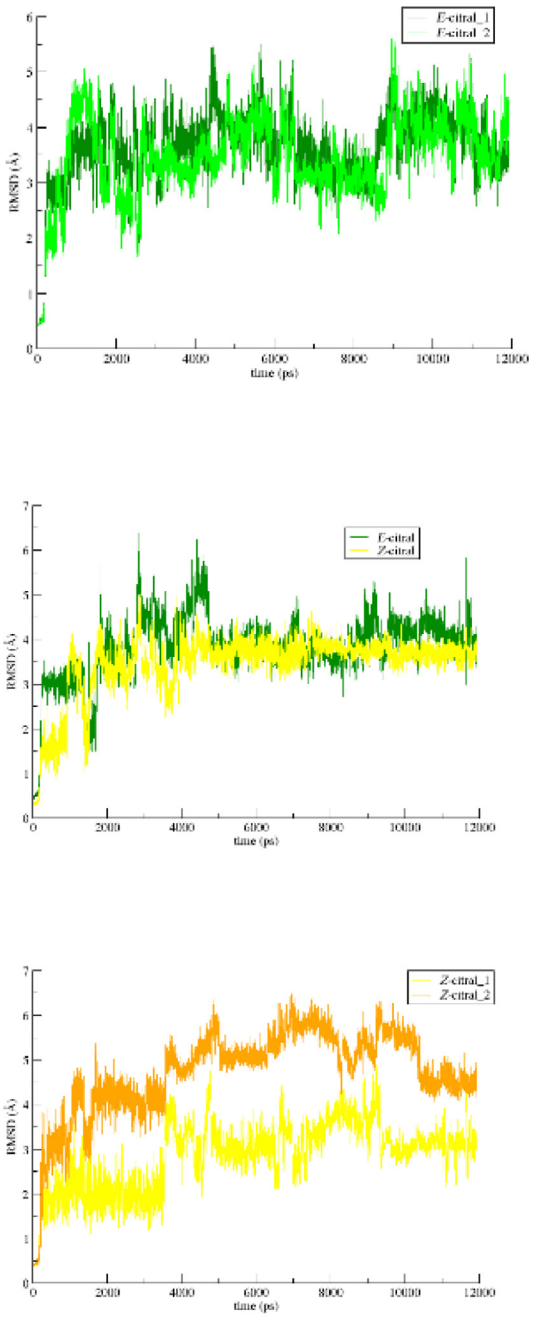

(b)

Fig. 7. Continued

Table 3
Binding free energies and their standard deviations (kcal/mole) resulting from MM/GBSA analysis of the inclusion compounds (guest:host stoichiometry 2:2) of i) *EE*/β-CD dimer (model determined by X-ray crystallography experiments), ii) *EZ*/β-CD dimer and iii) *ZZ*/β-CD dimer (models generated by Docking analysis).

	EE/βCD		*EZ*/βCD		*ZZ*/βCD	
	E-citral_1	*E-citral_1*	*E-citral*	*Z-citral*	*Z-citral_1*	*Z-citral_2*
ΔE_{vdW}	-28.4 ± 2.3	-27.8 ± 2.4	-27.0±2.6	-28.3±2.6	-27.5±2.8	-28.0±3.2
ΔE_{ele}	-2.7 ± 2.3	-2.7 ± 3.0	-2.8±2.5	-5.9±4.6	-2.3±1.9	-4.3±3.6
ΔE_{GB}	14.4 ± 2.4	14.1 ± 2.9	13.5±2.8	17.5±4.3	13.0±2.5	15.7±3.4
ΔE_{surf}	-3.7 ± 0.2	-3.6 ± 0.2	-3.5±0.3	-3.6±0.2	-3.5±0.2	-3.6±0.2
ΔG_{gas}	-31.1 ± 3.3	-30.6 ± 3.9	-29.7±4.0	-34.2±5.2	-30.0±3.8	-31.9±4.4
ΔG_{solv}	10.7 ± 2.2	10.4 ± 2.8	10.0±2.6	13.9±4.3	9.5±2.3	12.2±3.3
$\Delta G_{(GB)}$	-20.4 ± 2.1	-20.1 ± 2.2	-19.7±2.4	-20.3±2.3	-20.6±2.3	-19.8±3.0
$T \cdot \Delta S$	-17.2 ± 1.9	-16.9 ± 2.7	-17.0±2.9	-17.7±2.1	-17.2±2.3	16.4±2.1
ΔG_{bind}	**-3.2 ± 2.8**	**-3.2 ± 3.5**	**-2.7±3.7**	**-2.6±3.2**	**-3.4±3.3**	**-3.3±3.6**

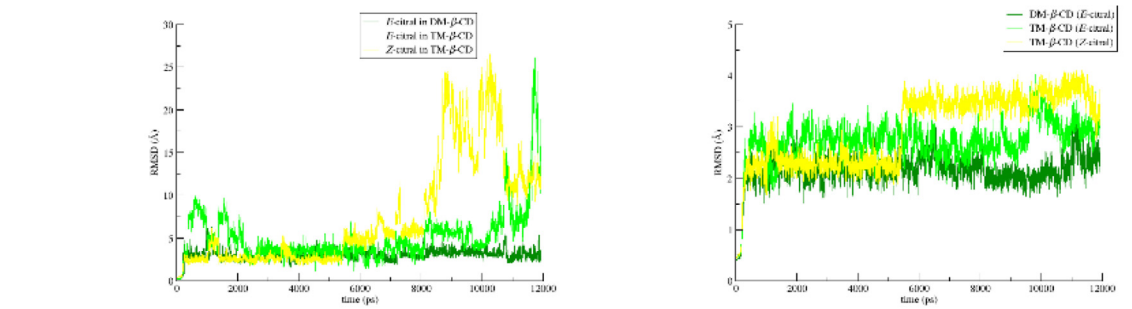

(a)

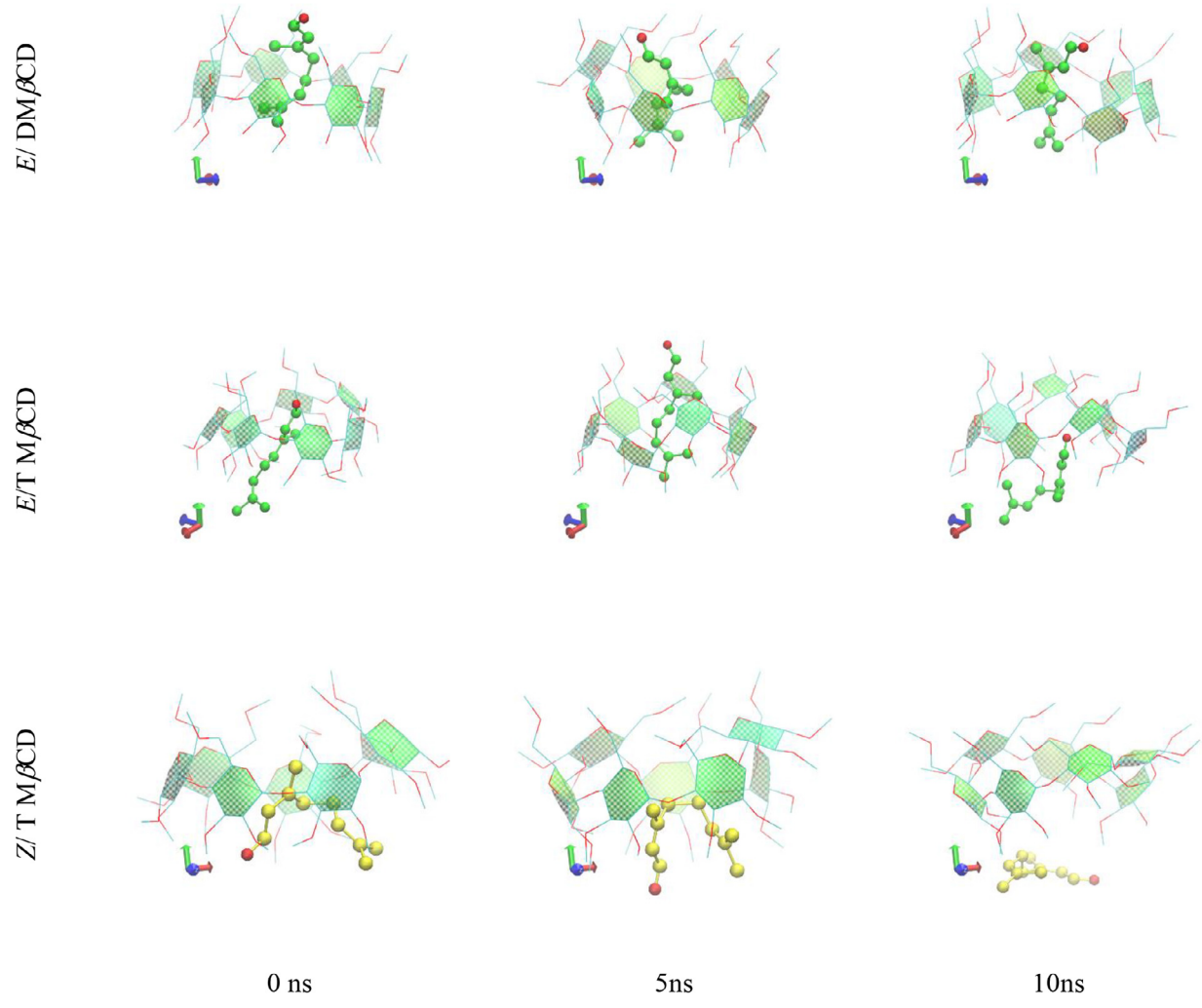

(b)

Fig. 8. **(a)** RMSD over time for all non-H atoms of the encapsulated citral isomers (left) and the respective hosts (right) in each one of the three inclusion complexes (*E*/DMβCD, *E*/TMβCD and *Z*/TMβCD) and **(b)** representative snapshots of *E*/DMβCD, *E*/TMβCD and *Z*/TMβCD inclusion complexes at 0ns, 5ns and 10 ns during the 12 ns simulation. *E*-citral (green) and *Z*-citral (yellow) are shown as CPKs and methylated CDs as paper chains. Images were rendered with VMD.

Table 4
Binding free energies and their standard deviations (kcal/mole) resulting from MM/GBSA analysis of the inclusion compounds of citral isomers with methylated cyclodextrins (guest:host stoichiometry 1:1).

	E/DMβCD	*E*/TMβCD	*Z*/TMβCD
ΔE_{vdW}	-25.17 ± 2.09	-23.48 ± 5.41	-15.46 ± 9.19
ΔE_{ele}	-0.16 ± 2.38	-4.42 ± 4.30	1.47 ± 2.17
ΔE_{GB}	6.92 ± 2.69	12.61 ± 4.10	3.68 ± 2.66
ΔE_{surf}	-3.35 ± 0.20	-3.21 ± 0.54	-2.08 ± 1.11
ΔG_{gas}	-25.33 ± 3.53	-27.90 ± 5.77	-13.99 ± 8.50
ΔG_{solv}	3.58 ± 2.61	9.40 ±4.13	1.61 ± 2.13
$\Delta G_{(GB)}$	-21.75 ± 2.09	-18.49 ± 4.79	-12.38 ± 7.74
$T\cdot\Delta S$	-16.39 ± 1.42	-16.87 ± 1.85	-11.71 ± 7.79
ΔG_{bind}	-5.36 ± 2.53	-1.62 ± 5.13	-0.67 ±11.09

of these intramolecular hydrogen bonds in the case of the permethylated TM-β-CD results to a higher host macrocycle distortion as it is shown in the RMSD plot for the host molecules (Fig. 8a, right). The rigid form of DM-β-CD facilitates the 'axial' accommodation of the *E*-citral with the aldehyde group of the guest projecting always through the primary rim and its aliphatic end located in the secondary rim of the host. Similar accommodation and dynamic behavior has been observed for the inclusion complexes of β-citronellol and geraniol in DM-β-CD [20–21]. On the other hand, the *E*/TMβCD inclusion complex is much less stable. The depth of immersion of the encapsulated *E*-citral inside the flexible host cavity varies significantly during the MD simulation and although the guest retains its axial accommodation, after the 10th ns, it escapes from the hydrophobic cavity through the secondary rim of the host entering in the aqueous environment (Fig. 8b). An even less stable inclusion complex is observed in the case of *Z*/TMβCD. *Z*-citral is found crystallographically with an occupancy factor of 0.3, in a bent conformation, partially encapsulated in the TMβCD cavity and accommodated 'equatorially' in the secondary rim of the host. MD simulations have shown that this inclusion mode is not stable as *Z*-citral abandons completely the host's cavity from its wide rim after the 8th ns (Fig. 8b).

The estimated binding affinities by MM/GBSA analysis (Table 4), for the three inclusion complexes with 1:1 guest:host stoichiometry, indicate that the stability of the inclusion complexes clearly follows the order: *E*/DMβCD > *E*/TMβCD > *Z*/TMβCD.

4. Conclusions

The crystal structures presented in this work confirm the inherent tendency of citral to form inclusion complexes in native α-, β- and methylated β-CDs similar to the previously reported inclusion complexes of other linear monoterpenes, like geraniol, citronellol and linalool, in CDs [20–22].

The inclusion complex of *cr*/α-CD crystallizes in the *P*1 space group forming channels along the *c*-axis. The *cr*/α-CD complex unit reveals the encapsulation of an *E*- or a *Z*-citral isomer (with occupancy of 0.4 and 0.6 respectively), which is accommodated axially in the interface of the formed head-to-head α-CD dimer (1:2 guest:host stoichiometry). The inclusion complex of *cr*/β-CD crystallizes in the *C*2 space group also forming channels along the *c*-axis. Two highly disordered guest molecules, both being *E*-citral isomers, are found axially accommodated inside a head-to-head β-CD dimeric cavity, with their aldehyde group located in the primary rim of the hosts (2:2 guest:host stoichiometry).

MD simulations based mainly on the determined crystal structures of the examined inclusion complexes, show that in a simulated aqueous environment, stable inclusion complexes of citral in both native α- and β-CD are formed. Interestingly, in both cases the encapsulated *Z*-citral seems to adopt a more bent conformation than E-citral and thus it has the ability to alternate its orientation in the wider β-CD cavity. MM/GBSA-calculations clearly indicated a higher binding affinity in the case of the *cr*/α-CD than the *cr*/β-CD inclusion complex. By comparing the binding affinities of the inclusion complexes of linear monoterpenes in β-CDs, that have been estimated by MM/GBSA calculations and for the same 2:2 guest:host stoichiometry revealed by crystallography [20–21], the ascending order of the ΔG values is: *citral*/β-CD < *geraniol*/β-CD < *citronellol*/β-CD.

Regarding the citral inclusion complexes in methylated β-CDs, both examined *cr*/DM-β-CD and *cr*/TM-β-CD crystallize in the orthorhombic $P2_12_12_1$ space group with 1:1 guest:host complex units arranged in a "head-to-tail" fashion forming antiparallel columns. Only the *E*-citral isomer is found inside the DM-β-CD with its aldehyde group protruding from the narrow rim of the host, whereas both *E*- and *Z*-citral isomers are present in the TM-β-CD having different occupancy factors, location and accommodation mode inside the host's cavity.

A structural comparison between citral inclusion complexes in native (α-CD and β-CD) and methylated (DM-β-CD and TM-β-CD) cyclodextrins reveals that in the crystalline state, the rigid cavity of β-CD and DM-β-CD favors, in a 2:2 and 1:1 host:guest stoichiometry respectively, the inclusion of the *E*-citral which adopts an extended conformation and it is accommodated 'axially' in it. On the other hand, the *Z*-citral isomer, that adopts a more bent conformation upon encapsulation in the hydrophobic CD cavity, is found only in the case of the *cr*/α-CD where the 1:2 guest:host stoichiometry provides the space to accommodate the bent *Z*-citral and in the case of the *cr*/TM-β-CD complex, where the bent *Z*-citral is found accommodated 'equatorially' near the wide secondary rim of the distorted host. MD simulations in aqueous environment reveal a stable inclusion complex of citral in DM-β-CD and a rather unstable in TM-β-CD, the ascending order of the binding affinities of these inclusion complexes as estimated by MM/GBSA calculations being: *Z*/TMβCD < *E*/TMβCD < *E*/DMβCD.

Credit author statement

Katerina Fourtaka: Conceptualization, Validation, Formal analysis, Investigation, Writing - Original Draft

Elias Christoforides: Conceptualization, Validation, Formal analysis, Investigation, Data Curation, Writing - Original Draft, Writing - Review & Editing, Visualization, Project administration

Pavlos Tzamalis: Formal analysis, Investigation, Data Curation

Kostas Bethanis: Conceptualization, Formal analysis, Investigation, Data Curation, Writing - Original Draft, Writing - Review & Editing, Supervision, Project administration

Declaration of Competing Interest

The authors declare that they have no known competing financial interests or personal relationships that could have appeared to influence the work reported in this paper.

Acknowledgments

We acknowledge support of this work by the project "INSPIRED-The National Research Infrastructures on Integrated Structural Biology, Drug Screening Efforts and Drug Target Functional Characterization" (Grant MIS 5002550), which is implemented under the Action "Reinforcement of the Research and Innovation Infrastructure", funded by the Operational Programme "Competitiveness, Entrepreneurship and Innovation" (Grant NSRF 2014–2020) and co-financed by Greece and the European Union (European Regional Development Fund).

Supplementary materials

Supplementary material associated with this article can be found, in the online version, at doi:10.1016/j.molstruc.2021.130169.

References

[1] A. Koziol, A. Stryjewska, T. Librowski, K. Salat, M. Gawel, A. Moniczewski, S. Lochynski, An overview of the pharmacological properties and potential applications of natural monoterpenes, Mini Rev. Med. Chem. 14 (2014) 1156–1168.

[2] J.R. Calo, P.G. Crandall, C.A. O'Bryan, S.C. Ricke, Essential oils as antimicrobials in food systems – a review, Food Control 54 (2015) 111–119, doi:10.1016/j.foodcont.2014.12.040.

[3] M. Perricone, E. Arace, M.R. Corbo, M. Sinigaglia, A. Bevilacqua, Bioactivity of essential oils: a review on their interaction with food components, Front. Microbiol. 6 (76) (2015), doi:10.3389/fmicb.2015.00076.

[4] A. Orchard, S. van Vuuren, Commercial essential oils as potential antimicrobials to treat skin diseases, Evid. Based Complement. Alternat. Med. 2017 (2017) 92.

[5] C.-C. Li, H.-F. Yu, C.-H. Chang, Y.-T. Liu, H.-T. Yao, Effects of lemongrass oil and citral on hepatic drug-metabolizing enzymes, oxidative stress, and acetaminophen toxicity in rats, J. Food Drug Anal. 26 (2018) 432–438, doi:10.1016/j.jfda.2017.01.008.

[6] W.-C. Lu, D.-W. Huang, C.-C.R. Wang, C.-H. Yeh, J.-C. Tsai, Y.-T. Huang, P.-H. Li, Preparation, characterization, and antimicrobial activity of nanoemulsions incorporating citral essential oil, J. Food Drug Anal. 26 (2018) 82–89, doi:10.1016/j.jfda.2016.12.018.

[7] E.C. Adukwu, M. Bowles, V. Edwards-Jones, H. Bone, Antimicrobial activity, cytotoxicity and chemical analysis of lemongrass essential oil (Cymbopogon flexuosus) and pure citral, Appl. Microbiol. Biotechnol. 100 (2016) 9619–9627, doi:10.1007/s00253-016-7807-y.

[8] G. Wadhwa, S. Kumar, L. Chhabra, S. Mahant, R. Rao, Essential oil–cyclodextrin complexes: an updated review, J. Incl. Phenom. Macrocycl. Chem. 89 (2017) 39–58, doi:10.1007/s10847-017-0744-2.

[9] G. Astray, C. Gonzalez-Barreiro, J.C. Mejuto, R. Rial-Otero, J. Simal-Gándara, A review on the use of cyclodextrins in foods, Food Hydrocoll. 23 (2009) 1631–1640. http://dx.doi.org/10.1016/j.foodhyd.2009.01.001.

[10] H. Matsuda, K. Ito, Y. Fujiwara, M. Tanaka, A. Taki, O. Uejima, H. Sumiyoshi, Complexation of various fragrance materials with 2-hydroxypropyl-β-cyclodextrin, Chem. Pharm. Bull. (Tokyo). 39 (1991) 827–830, doi:10.1248/cpb.39.827.

[11] G. Decock, D. Landy, G. Surpateanu, S. Fourmentin, Study of the retention of aroma components by cyclodextrins by static headspace gas chromatography, J. Incl. Phenom. Macrocycl. Chem. 62 (2008) 297–302, doi:10.1007/s10847-008-9471-z.

[12] S. Phunpee, U. Ruktanonchai, H. Yoshii, S. Assabumrungrat, A. Soottitantawat, Encapsulation of lemongrass oil with cyclodextrins by spray drying and its controlled release characteristics, Biosci. Biotechnol. Biochem. 81 (2017) 1–6.

[13] T. Ishiguro, Y. Sakata, H. Arima, D. Iohara, M. Anraku, K. Uekama, F. Hirayama, Release control of fragrances by complexation with β-cyclodextrin and its derivatives, J. Incl. Phenom. Macrocycl. Chem. (2018), doi:10.1007/s10847-018-0825-x.

[14] C.A. Campos, B.S. Lima, G.G.G. Trindade, E.P.B.S.S. Souza, D.S.A. Mota, L. Heimfarth, J.S.S. Quintans, L.J. Quintans-Júnior, E.M. Sussuchi, V.H.V. Sarmento, F.M.S. Carvalho, R.N. Marreto, R.M.R. Costa, R.S. Nunes, A.A.S. Araújo, S. Shanmugam, P. Thangaraj, Anti-hyperalgesic and anti-inflammatory effects of citral with β-cyclodextrin and hydroxypropyl-β-cyclodextrin inclusion complexes in animal models, Life Sci. 229 (2019) 139–148, doi:10.1016/j.lfs.2019.05.026.

[15] Z. Xiao, N. Feng, G. Zhu, Y. Niu, Preparation and application of citral–monochlorotriazine-β-cyclodextrin inclusion complex nanocapsule, J. Text. Inst. 107 (2016) 64–71, doi:10.1080/00405000.2014.1000579.

[16] U.R. Ruktanonchai, W. Srinuanchai, S. Saesoo, I. Sramala, S. Puttipipatkhachorn, A. Soottitantawat, Encapsulation of citral isomers in extracted lemongrass oil with cyclodextrins: molecular modeling and physicochemical characterizations, Biosci. Biotechnol. Biochem. 75 (2011) 2340–2345, doi:10.1271/bbb.110523.

[17] G. Zhu, N. Feng, Z. Xiao, R. Zhou, Y. Niu, Production and pyrolysis characteristics of citral–monochlorotriazinyl-β-cyclodextrin inclusion complex, J. Therm. Anal. Calorim. 120 (2015) 1811–1817, doi:10.1007/s10973-015-4498-z.

[18] P. Wongpituk, B. Nutho, W. Panman, N. Kungwan, P. Wolschann, T. Rungrotmongkol, N. Nunthaboot, Structural dynamics and binding free energy of neral-cyclodextrins inclusion complexes: molecular dynamics simulation, Mol. Simul. 43 (2017) 1356–1363, doi:10.1080/08927022.2017.1356458.

[19] Z. Aytac, A. Celebioglu, I.Z. Yildiz, T. Uyar, Efficient encapsulation of citral in fast-dissolving polymer-free electrospun nanofibers of cyclodextrin inclusion complexes: high thermal stability, longer shelf-life, and enhanced water solubility of citral, Nanomaterials 8 (2018), doi:10.3390/nano8100793.

[20] K. Fourtaka, E. Christoforides, D. Mentzafos, K. Bethanis, Crystal structures and molecular dynamics studies of the inclusion compounds of β-citronellol in β-cyclodextrin, heptakis(2,6-di-O-methyl)-β-cyclodextrin and heptakis(2,3,6-tri-O-methyl)-β-cyclodextrin, J. Mol. Struct. 1161 (2018) 1–8, doi:10.1016/j.molstruc.2018.02.037.

[21] E. Christoforides, K. Fourtaka, A. Andreou, K. Bethanis, X-ray crystallography and molecular dynamics studies of the inclusion complexes of geraniol in β-cyclodextrin, heptakis (2,6-di-O-methyl)-β-cyclodextrin and heptakis (2,3,6-tri-O-methyl)-β-cyclodextrin, J. Mol. Struct. 1202 (2020) 127350, doi:10.1016/j.molstruc.2019.127350.

[22] M. Ceborska, Structural investigation of solid state host/guest complexes of native cyclodextrins with monoterpenes and their simple derivatives, J. Mol. Struct. 1165 (2018) 62–70, doi:10.1016/j.molstruc.2018.03.114.

[23] Bruker-AXS, SAINT, Madison, Wisconsin, USA, 2013.

[24] G.M. Sheldrick, Bruker-AXS, SADABS, Madison, Wisconsin, USA, 2012.

[25] G.M. Sheldrick, Experimental phasing with SHELXC/D/ E: combining chain tracing with density modification, Acta Crystallogr. Sect. D. 66 (2010) 479–485, doi:10.1107/S0907444909038360.

[26] Y. Takashima, K. Sakamoto, Y. Oizumi, H. Yamaguchi, S. Kamitori, A. Harada, Complex formation of cyclodextrins with various thiophenes and their polymerization in water: preparation of poly-pseudo-rotaxanes containing poly(thiophene)s, J. Incl. Phenom. Macrocycl. Chem. 56 (2006) 45–53, doi:10.1007/s10847-006-9059-4.

[27] P.T. Beurskens, G. Beurskens, R. de Gelder, S. Garcia-Granda, R.O. Gould, J.M.M. Smits, The DIRDIF2008 Program System, Crystallography Laboratory, University of Nijmegen, The Netherlands., 2008.

[28] G.M. Sheldrick, Crystal structure refinement with SHELXL, Acta Crystallogr. Sect. C Struct. Chem. 71 (2015) 3–8, doi:10.1107/S2053229614024218.

[29] C.B. Hübschle, G.M. Sheldrick, B. Dittrich, ShelXle: a Qt graphical user interface for SHELXL, J. Appl. Crystallogr. 44 (2011) 1281–1284, doi:10.1107/S0021889811043202.

[30] A.W. Schuttelkopf, D.M.F. van Aalten, PRODRG: a tool for high-throughput crystallography of protein-ligand complexes, Acta Crystallogr. D Biol. Crystallogr. 60 (2004) 1355–1363, doi:10.1107/S0907444904011679.

[31] A. Thorn, B. Dittrich, G.M. Sheldrick, Enhanced rigid-bond restraints, Acta Crystallogr. A. 68 (2012) 448–451, doi:10.1107/S0108767312014535.

[32] C.F. Macrae, I.J. Bruno, J.A. Chisholm, P.R. Edgington, P. McCabe, E. Pidcock, L. Rodriguez-Monge, R. Taylor, J. van de Streek, P.A. Wood, Mercury CSD 2.0 – new features for the visualization and investigation of crystal structures, J. Appl. Crystallogr. 41 (2008) 466–470, doi:10.1107/S0021889807067908.

[33] O.V. Dolomanov, L.J. Bourhis, R.J. Gildea, J.A.K. Howard, H. Puschmann, OLEX2: a complete structure solution, refinement and analysis program, J. Appl. Crystallogr. 42 (2009) 339–341, doi:10.1107/S0021889808042726.

[34] O. Trott, A.J. Olson, AutoDock Vina: improving the speed and accuracy of docking with a new scoring function, efficient optimization, and multithreading, J. Comput. Chem. 31 (2010) 455–461, doi:10.1002/jcc.21334.

[35] R. Salomon-Ferrer, D.A. Case, R.C. Walker, An overview of the Amber biomolecular simulation package, Wiley Interdiscip. Rev. Comput. Mol. Sci. 3 (2012) 198–210, doi:10.1002/wcms.1121.

[36] K.N. Kirschner, A.B. Yongye, S.M. Tschampel, J. Gonzalez-Outeirino, C.R. Daniels, B.L. Foley, R.J. Woods, GLYCAM06: a generalizable biomolecular force field. Carbohydrates, J. Comput. Chem. 29 (2008) 622–655, doi:10.1002/jcc.20820.

[37] C. Cezard, X. Trivelli, F. Aubry, F. Djedaini-Pilard, F.-Y. Dupradeau, Molecular dynamics studies of native and substituted cyclodextrins in different media: 1. Charge derivation and force field performances, Phys. Chem. Chem. Phys. PCCP. 13 (2011) 15103–15121, doi:10.1039/c1cp20854c.

[38] J. Wang, W. Wang, P.A. Kollman, D.A. Case, Automatic atom type and bond type perception in molecular mechanical calculations, J. Mol. Graph. Model. 25 (2006) 247–260, doi:10.1016/j.jmgm.2005.12.005.

[39] V. Kräutler, W.F. van Gunsteren, P.H. Hünenberger, A fast SHAKE algorithm to solve distance constraint equations for small molecules in molecular dynamics simulations, J. Comput. Chem. 22 (2001) 501–508, doi:10.1002/1096-987X(20010415)22:5⟨501::AID-JCC1021⟩3.0.CO;2-V.

[40] K. Bethanis, E. Christoforides, F. Tsorteki, K. Fourtaka, D. Mentzafos, Structural studies of the inclusion compounds of α-naphthaleneacetic acid in heptakis(2,6-di-O-methyl)-β-Cyclodextrin and heptakis(2,3,6-tri-O-methyl)-β-Cyclodextrin by X-ray crystallography and molecular dynamics, J. Incl. Phenom. Macrocycl. Chem. 92 (2018) 157–171, doi:10.1007/s10847-018-0824-y.

[41] D.R. Roe, T.E. 3rd Cheatham, PTRAJ and CPPTRAJ: software for processing and analysis of molecular dynamics trajectory data, J. Chem. Theory Comput. 9 (2013) 3084–3095, doi:10.1021/ct400341p.

[42] W. Humphrey, A. Dalke, K. Schulten, VMD: visual molecular dynamics, J. Mol. Graph. 14 (1996) 27–28 33–8.

[43] B.R. 3rd Miller, T.D.J. McGee, J.M. Swails, N. Homeyer, H. Gohlke, A.E. Roitberg, MMPBSA.py: an efficient program for end-state free energy calculations, J. Chem. Theory Comput. 8 (2012) 3314–3321, doi:10.1021/ct300418h.

[44] C.R. Groom, I.J. Bruno, M.P. Lightfoot, S.C. Ward, The Cambridge structural database, Acta Crystallogr. Sect. B. 72 (2016) 171–179, doi:10.1107/S2052520616003954.

[45] S. Choi, W. Frank, H. Ritter, Novel polymerization of diethyl fumarate and maleate in aqueous media via cyclodextrin-complexes, Spec. Issue Honour John Ebdon. 66 (2006) 149–156. 10.1016/j.reactfunctpolym.2005.07.013.

[46] C. Sicard-Roselli, B. Perly, G.L.e Bas, The respective benefits of x-ray crystallography and nmr for the structural determination of the inclusion complex between butyl-isothiocyanate and alpha-cyclodextrin, J. Incl. Phenom. Macrocycl. Chem. 39 (2001) 333–337, doi:10.1023/A:1011163608747.

[47] D. Mentzafos, I.M. Mavridis, G.L.e Bas, G. Tsoucaris, Structure of the 4-ıt tert-butylbenzyl alcohol–β-cyclodextrin complex. Common features in the geometry of β-cyclodextrin dimeric complexes, Acta Crystallogr. Sect. B. 47 (1991) 746–757, doi:10.1107/S010876819100366X.

[48] M. Ceborska, Structural investigation of the β-cyclodextrin complexes with linalool and isopinocampheol – influence of monoterpenes cyclicity on the host–guest stoichiometry, Chem. Phys. Lett. 651 (2016) 192–197, doi:10.1016/j.cplett.2016.03.051.

[49] M. Ceborska, K. Szwed, M. Asztemborska, M. Wszelaka-Rylik, E. Kicińska, K. Suwińska, Study of β-cyclodextrin inclusion complexes with volatile molecules geraniol and α-terpineol enantiomers in solid state and in solution, Chem. Phys. Lett. 641 (2015) 44–50, doi:10.1016/j.cplett.2015.10.018.

[50] R.H. Vyas, C.J.E. Kempster, The low- and high-temperature phases of tris(ethylene terephthalate), Acta Crystallogr. Sect. A. 40 (C276) (1984), doi:10.1107/S0108767384091765.

[51] M.R. Caira, S.A. Bourne, B. Mzondo, Encapsulation of the antioxidant R-(+)-α-lipoic acid in permethylated α- and β-cyclodextrins: thermal and X-ray structural characterization of the 1:1 inclusion complexes, Molecules 22 (2017), doi:10.3390/molecules22060866.

[52] D.L. Cruickshank, N.M. Rougier, V.J. Maurel, R.H. de Rossi, E.I. Buján, S.A. Bourne, M.R. Caira, Permethylated β-cyclodextrin/pesticide complexes: X-ray structures and thermogravimetric assessment of kinetic parameters for complex dissociation, J. Incl. Phenom. Macrocycl. Chem. 75 (2013) 47–56, doi:10.1007/s10847-012-0145-5.

[53] K. Harata, K. Uekama, M. Otagiri, F. Hirayama, The structure of the cyclodextrin complex. XVI. Crystal structure of Heptakis(2,3,6-tri-O-methyl)-β-cyclodextrin-p-Iodophenol (1 : 1) complex tetrahydrate, Bull. Chem. Soc. Jpn. 56 (1983) 1732–1736, doi:10.1246/bcsj.56.1732.

[54] N.S. Stellenboom, Synthesis and Inclusion Studies of Stable Allicin Mimics as Novel Antimicrobial Agents, Doctor of Philosophy, University of Cape Town, 2008.

[55] M.R. Caira, D. Cruickshank, S.A. Bourne, Solid-state structures and thermal properties of inclusion complexes of the phenylurea herbicide cycluron with permethylated cyclodextrins, ARKIVOC 2011 (2011) 103–115, doi:10.3998/ark.5550190.0012.709.